

## The crystal structure of norrishite, $\text{KLiMn}_2^{3+}\text{Si}_4\text{O}_{12}$ : An oxygen-rich mica

PAUL L. TYRNA, STEPHEN GUGGENHEIM

Department of Geological Sciences, University of Illinois at Chicago, Chicago, Illinois 60680 U.S.A.

### ABSTRACT

The crystal structure of norrishite-*1M* was refined by least squares using 649 single crystal X-ray intensities to an  $R$  value of 0.078 ( $R_w = 0.098$ ). The structure is monoclinic ( $C2/m$ ) with cell parameters:  $a = 5.289(3)$  Å,  $b = 8.914(3)$  Å,  $c = 10.062(7)$  Å,  $\beta = 98.22(5)^\circ$ . The O atom [O(4)] usually associated with  $\text{H}^+$  in an ideal mica is highly under-saturated (about 1.7 e.v.u.) based on weighted Pauling bond-strength calculations. Hence, the octahedrally coordinated  $\text{Mn}^{3+}$  cation is displaced from the polyhedral center toward the O(4)-O(4) shared edge [ $\text{Mn}-\text{O}(4) = 1.855$  Å vs.  $\text{Mn}-\text{O}(3) = 2.023$  Å]. The asymmetrical displacement of M(2) toward O(4) produces a charge deficiency on the apical O atom [O(3)], which is balanced by a short Si-O(3) distance of 1.571 Å.

Jahn-Teller distortions associated with  $\text{Mn}^{3+}$  are consistent with the distortions from electrostatic effects; octahedra are lengthened approximately parallel to [100] and shortened with respect to [010] and [001]. Relative lengths of shared octahedral edges are similar to those observed in dioctahedral micas and are the result of the size and charge differences between M(1) and M(2) ( $\text{Li}^+$  vs.  $\text{Mn}^{3+}$ ). These distortions, in addition to the relatively large ionic radii of Mn and Li, extend the lateral dimensions of the octahedral sheet and minimize tetrahedral rotation ( $\alpha = 0.6^\circ$ ), thereby forming a hexagonal interlayer cation site. A narrow interlayer region (3.275 Å) results, in part, from coulombic interactions between O(4) and K. Displacement of Si toward O(3) may be due, in part, to Si-Si repulsion across the interlayer.

### INTRODUCTION

Norrishite, approximately  $\text{K}_{0.98}\square_{0.02}(\text{LiMn}_{1.98}^{3+})(\text{Si}_{3.91}\text{Al}_{0.09})\text{O}_{12}$ , is a trioctahedral mica presently limited in occurrence to the Hoskins mine near Grenfell, New South Wales, Australia. The locality consists of a steeply dipping metamorphosed stratiform unit that has been interpreted as submarine exhalative in origin (Ashley, 1986). Norrishite occurs as lustrous brown-black flakes up to 1 mm across with perfect {001} cleavage, and it resembles manganese biotite in hand specimens. The lack of Fe in norrishite is believed to be related to the different solubilities and oxidation potentials of Fe and Mn, which presumably caused Mn-Fe segregation in the deposit; Li was probably derived from precursor phyllosilicate-rich muds and precipitates. Chemical composition, optical, and physical properties were given by Eggleton and Ashley (1989).

Norrishite is anhydrous; it is more properly classified as a mica with O in the site normally occupied by OH, which for the purposes of this paper will be referred to as an "oxymica." The absence of these components makes norrishite a chemically unique end-member species. The existence of oxymicas, both natural and synthetic, was proposed previously. Larson et al. (1937), in an analysis of biotite from Tertiary volcanic rocks, suggested that a decrease in OH content (deprotonization) may be related

to the amount of  $\text{Fe}_2\text{O}_3$  present, with the relationship governed by the reaction:  $2\text{FeO} + \text{H}_2\text{O} = \text{Fe}_2\text{O}_3 + \text{H}_2$ . Similarly, Wones (1963), in a study of the physical properties of synthetic biotite, suggested the same reaction. More recently, Ohta et al. (1982) refined the structures of coexisting *1M* and *2M*<sub>1</sub> biotite with O in the OH site (henceforth to be referred to as "oxybiotite") and related partial hydrogenation to increased O-O (shared) edge lengths and an increased interlayer separation. Norrishite, because it represents an end-member O-rich mica, affords an opportunity for a more detailed analysis of the effects of an O component on the atomic structure.

### EXPERIMENTAL

Norrishite from near Grenfell, New South Wales, Australia (Australian National University #39901-C) was used in this study. The composition of similar material is given by Eggleton and Ashley (1989) as  $(\text{K}_{0.97}\text{Na}_{0.005})\text{-}(\text{LiMn}_{1.96}^{3+}\text{Mg}_{0.025}\text{Ti}_{0.01}\text{Al}_{0.005})_{\Sigma=3.0}(\text{Si}_{3.94}\text{Al}_{0.06})\text{O}_{12.11}$ .

Examination of 87 crystals by the precession method produced one crystal (approximately 0.25 mm × 0.25 mm × 0.07 mm) that was considered suitable for measurement of data for refinement. This sample exhibited considerable mosaic spread and traces of powder diffraction rings, sometimes with as much as 16° of arc. However, there was only a relatively minor amount of streak-

TABLE 1. Atomic coordinates and thermal parameters for norrishite

Atom	x	y	z	B <sub>iso</sub> *	β <sub>11</sub>	β <sub>22</sub>	β <sub>33</sub>	β <sub>12</sub>	β <sub>13</sub>	β <sub>23</sub>
K	0	1/2	0	2.8(2)	0.017(2)	0.0050(5)	0.0077(6)	0	0.0020(8)	0
M(1)	0	0	1/2	1.0(5)	0.009(6)	0.004(2)	0.004(2)	0	0.002(2)	0
M(2)	0	0.3472(3)	1/2	1.22(8)	0.0039(6)	0.0011(2)	0.0038(2)	0	0.0011(3)	0
T	0.0629(4)	0.1707(3)	0.2270(3)	1.29(9)	0.0044(8)	0.0012(3)	0.0040(3)	0.0000(3)	0.0008(3)	0.0000(2)
O(1)	0.045(2)	0	0.167(1)	1.5(3)	0.010(3)	0.0019(9)	0.005(1)	0	0.001(1)	0
O(2)	0.297(1)	0.2486(8)	0.1615(7)	2.2(2)	0.007(2)	0.0040(7)	0.0041(6)	-0.0025(9)	0.0006(8)	0.0001(6)
O(3)	0.108(1)	0.1787(7)	0.3853(7)	1.0(2)	0.005(2)	0.0014(6)	0.0044(6)	0.0002(7)	0.0015(9)	-0.0002(4)
O(4)	0.109(2)	1/2	0.396(1)	1.7(3)	0.009(3)	0.0015(8)	0.005(1)	0	0.002(1)	0

Note: For Table 1 and subsequent tables, numbers in parentheses represent one esd of least units cited. β<sub>*y*</sub> = anisotropic temperature factor of the form exp[-Σ<sub>*i*</sub>Σ<sub>*j*</sub>β<sub>*ij*</sub>h<sub>*i*</sub>h<sub>*j*</sub>]

\* B<sub>iso</sub> = isotropic temperature factor, refined.

ing parallel to *c*\* along *k* ≠ 3*n* reflections, indicating minor stacking disorder. Examination of zero and upper level photographs indicated the presence of reflections of the type *h* + *k* = 2*n*, which define a *C*-centered cell. On the basis of cell geometry and an apparent mirror plane and twofold axis, space group *C2/m*, which is typical for the *IM* polytype, was assumed.

An automated Krisel-controlled four-circle diffractometer with a graphite monochromator and MoKα radiation was used for data measurement. Cell parameters were refined (MoKα<sub>1</sub> = 0.70930 Å) from 160 reflections (20 reflections in eight octants) to yield the following: *a* = 5.289(3) Å, *b* = 8.914(4) Å, *c* = 10.062(7) Å, β = 98.22(5)°. A total of 2303 reflections were measured over the range 2θ = 2°–70° at a scan rate of 0.5°/min, with a 2° scan window and a 10 s background time. To check system and crystal stability, three standard reflections were monitored after every 57 reflections. The data were corrected for Lorentz and polarization effects, and absorption effects were empirically determined using ψ scans (North et al., 1968). The ψ scan data showed maximum intensity variations of 35%. Reflections with intensity (*I*) less than 6σ were considered to be unobserved. The standard deviation of the intensity, σ(*I*) is equal to [C + 0.25(*t<sub>c</sub>*/*t<sub>b</sub>*)<sup>2</sup>(B<sub>1</sub> + B<sub>2</sub>) + (*pI*)<sup>2</sup>]<sup>1/2</sup>, where *C* is the total integrated counts in time *t<sub>c</sub>*, B<sub>1</sub> and B<sub>2</sub> are the background counts in time *t<sub>b</sub>*, and *p* is arbitrarily chosen as 0.03. Reflections were symmetry averaged to yield 692 independent data. Of these, 43 *hkO* reflections were removed because ψ scans do not accurately account for dispersion effects close to the (001) plane of micas.

Initial parameters for the refinement were taken from lepidolite-*IM* (Guggenheim, 1981). The crystallographic least-squares program ORFLS (Busing et al., 1962) was used. Scattering factors were from Cromer and Mann (1968) and all atoms were considered to be half-ionized. The initial data were measured in two sets, requiring the use of separate scale factors. Structure factor calculations for *k* ≠ 3*n* reflections were made also with a separate scale factor (in each set) to reduce the effect of the minor streaking from partial stacking disorder, resulting in a total of four scale factors.

Throughout the first cycles of refinement, Li was allocated to M(1) and Mn to M(2), and all reflections were

given unit weight. Atom positions and scale factors were varied first, followed by the isotropic temperature factors. The *R* (*R* = Σ|*F<sub>o</sub>* - *F<sub>c</sub>*|/Σ|*F<sub>o</sub>*|) value decreased to 0.129 after the completion of six cycles. Anomalous scattering factors were then applied to Mn and K, and unit weights were replaced with several different weighing schemes. These procedures did not reduce the *R* value further and thus, were not used in the final cycles. A second model was refined using the same initial parameters but excluding Li from the structure in order to test for the presence of Li. The *R* and *R<sub>w</sub>* (*R<sub>w</sub>* = [Σ *w*(|*F<sub>o</sub>*| - |*F<sub>c</sub>*|)<sup>2</sup>/Σ *w*|*F<sub>c</sub>*|<sup>2</sup>]<sup>1/2</sup>) values remained high (0.141 and 0.162, respectively) and the model was abandoned. The initial model was then examined by computing electron density and difference electron density Fourier maps. For the latter, no significant peaks were observed, indicating that the model is accurate. As a further test, however, the M(1) site scale factor was allowed to vary and the other parameters were held constant. No significant changes in *R* values occurred, further suggesting that the initial model was correct. Finally, anisotropic temperature factors were introduced and *R* and *R<sub>w</sub>* decreased to 0.078 and 0.097, respectively, values that were judged acceptable considering the quality of the crystal. Final atomic coordinates and temperature parameters, interatomic bond distances as derived from Busing et al. (1964), orientations of thermal ellipsoids, and observed and calculated structure amplitudes are given in Tables 1, 2, 3,<sup>1</sup> and 4, respectively.

## DISCUSSION

An analysis of the deviations of bond lengths in norrishite from the ideal trioctahedral structure is complicated by the fact that polyhedral distortions, especially those in the octahedral sheet, are the result of three independent crystal chemical phenomena: (1) a large asymmetrical displacement of the M(2) cation in response to the presence of O in the site normally occupied by OH [O(4)], (2) elongation of octahedra approximately parallel

<sup>1</sup> A copy of Tables 3 and 4 may be ordered as Document AM-91-448 from the Business Office, Mineralogical Society of America, 1130 Seventeenth Street NW, Suite 330, Washington, DC 20036, U.S.A. Please remit \$5.00 in advance for the microfiche.

TABLE 2. Calculated bond lengths and angles

Bond lengths (Å)		Bond angles (°)		
		About T		
T-O(1)	1.633(5)	O(1)-O(2)'	2.592(9)	104.8(4)
O(2)'	1.638(7)	O(2)	2.592(8)	105.2(5)
O(2)	1.636(7)	O(3)	2.68(1)	113.8(4)
O(3)	1.571(8)	O(2)-O(2)'	2.6446(1)	108.1(3)
		O(3)	2.65(1)	111.7(4)
mean	1.620	O(2)-O(3)	2.66(1)	112.6(3)
		mean	2.638	mean 108.7
K-O(1)x2	3.12(1)			
O(1)x2	3.12(1)			
O(2)x2	3.064(8)			
O(2)x2	3.029(8)			
mean	3.071			
		shared		About M(1)
M(1) O(3)x4	2.092(6)	O(3)-O(3)x2	2.71(1)	80.8(3)
O(4)x2	2.18(1)	O(4)x4	2.94(1)	86.9(3)
mean	2.121	mean	2.863	
		unshared		
		O(3) O(3)x2	3.19(1)	99.2(3)
		O(4)x4	3.10(1)	93.1(2)
		mean	3.13	
		shared		About M(2)
M(2) O(3)x2	2.023(6)	O(3)-O(3)	2.71(1)	84.1(4)
O(3)'x2	2.233(7)	O(3)'x2	2.86(1)	84.2(3)
O(4)x2	1.855(7)	O(4)-O(3)'x2	2.94(1)	91.4(4)
		O(4)	2.52(2)	85.5(5)
mean	2.037	mean	2.805	
		unshared		
		O(3)-O(3)'x2	2.934(5)	87.0(3)
		O(4)x2	2.866(6)	95.1(3)
		O(4)-O(3)'x2	3.08(1)	97.3(4)
		mean	2.96	

to [100] due to the Jahn-Teller effect, and (3) dioctahedral-like distortions resulting from the size and charge differences between M(1) and M(2) ( $\text{Li}^+$  vs.  $\text{Mn}^{3+}$ ). In addition, the substitution of O in O(4) affects the spacing between 2:1 layers, which is discussed separately.

### Effect of the O component

The octahedral sheet is shown projected onto (001) in Figure 1. Similar to most other trioctahedral structures, the M(1) site is larger than M(2), mean bond lengths being 2.12 Å and 2.04 Å, respectively. The M(1)-O(4) bond distance is greater [2.18(1) Å vs. 2.092(6) Å] than M(1)-O(3), and M(2)-O(3) is considerably greater [2.023 Å vs. 1.855(7) Å] than M(2)-O(4). The difference in the latter bond lengths can be directly attributed to the presence of the O in O(4). In the ideal trioctahedral mica structure, two monovalent ( $\text{F}^-$  or  $\text{OH}^-$ ) anions compose an edge shared by two adjacent M(2) octahedra [labeled O(4)-O(4) in Fig. 1]. The effect of two divalent ( $\text{O}^{2-}$ ) anions in these sites in norrishite is an increased electrostatic attraction between M(2) and O(4), resulting in a large asymmetrical displacement of M(2) in a direction perpendicular to the O(4)-O(4) edge. A similar shift is observed in "oxybitite" (Ohta et al., 1982), although, because norrishite is an end-member with respect to the O in O(4) and the M(2) cation is trivalent, the magnitude of displacement is unique among the trioctahedral micas. The attraction

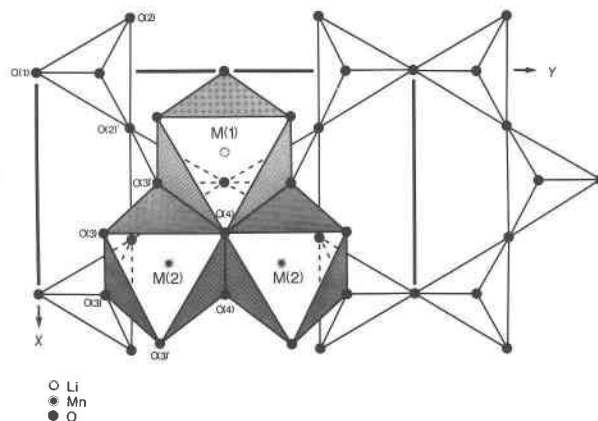


Fig. 1. Projection of norrishite structure down  $c^*$ . Note that the M(2) cations are not centered in the polyhedron.

between M(2) and O(4) apparently overcomes the Mn-Mn repulsion [Mn-Mn distance = 2.724(5) Å] across the O(4)-O(4) shared edge. Each O(4) anion is bonded to the three cations in surrounding octahedra, and the direction of movement of O(4) is the resultant of the three directional cation to anion bond forces. Because the O(4)-O(4) edge is parallel to the weaker Li-O(4) bond and perpendicular to the resultant of the  $\text{Mn}^{3+}$ -O(4) bonds, the O(4) anions are shifted closer to each other along their shared edge. The O(4)-O(4) edge, therefore, is shortened and acts as a more efficient electrostatic shield to the neighboring  $\text{Mn}^{3+}$  cations. The shared octahedral edge [2.52(2) Å] in norrishite deviates from the range of values (2.6 Å to 2.9 Å) for shared edge lengths in trioctahedral structures (Bailey, 1984). The short shared edge contrasts with the general trend in trioctahedral micas in which O-O shared edges are longer than O-(F,OH) or (OH,F)-(F,OH) edges, due to greater anion-anion repulsion (McCauley et al., 1973).

It is clear that  $\text{Mn}^{3+}$ - $\text{Mn}^{3+}$  repulsion is a significant factor in the net displacement of M(2). The limit of approach between neighboring M(2) cations is reflected in the bond valence sum (Table 5) for O(4). Although such valence sums cannot rigorously be applied to structures exhibiting strong Jahn-Teller distortions (Brown, 1977), it is nevertheless useful to evaluate bond valences in this manner to determine approximate bond valence sums. Valence sums for O(1), O(2), and O(3) are close to the ideal value of 2.0, whereas that of O(4) is 1.69 electrostatic valence units (e.v.u.), indicating that O(4) is considerably undersaturated with respect to the other anions. In order to satisfy this local valence imbalance, a shorter M(2)-O(4) bond is required. Thus, the overall displacement of M(2) reflects the balance between the attractive forces between M(2) and O(4), and the repulsive forces between M(2)-M(2) and O(4)-O(4).

### Jahn-Teller effects

The controls on the general arrangement of anions in the octahedra are consistent with the Jahn-Teller effect

TABLE 5. Bond valence sums (e.v.u.) for norrishite

	K	K'	M(1)	M(2)	M(2)'	T	T'	$\Sigma s$
O(1)	0.08 0.08 0.08 0.08	0.08 0.08 0.08 0.08				0.97	0.97	2.10
O(2)	0.09 0.09 0.09 0.09	0.09 0.09 0.09 0.09				0.96	0.96	2.10
O(2)	0.10 0.10 0.10 0.10	0.10 0.10 0.10 0.10				0.96	0.96	2.12
O(3)			0.18 0.18 0.18 0.18	0.48 0.48 0.28 0.28	0.28 0.28 0.48 0.48	1.15		2.09
O(4)			0.15 0.15 0.15	0.77 0.77 0.77	0.77 0.77			1.69
$\Sigma s$	1.08		1.02	3.06	3.06	4.04		

Note: Valence sums are calculated using  $s = [R/R_0]^{-N}$ , where  $s$  is the bond valence (e.v.u.),  $R$  is the observed bond length,  $R_0$ , and  $-N$  are empirical parameters for cation-O bond curves from Brown and Shannon (1973).  $K'$ ,  $M(2)'$  and  $T'$ : The prime represents a symmetry equivalent atom.

associated with trivalent Mn. The  $Mn^{3+}$  cation is stable in a distorted octahedral environment, where one of the four 3d electrons may reside in either one of the two  $e_g$  orbitals ( $d_{x^2-y^2}$ ,  $d_{z^2}$ ). Although it is not possible to predict which distortion will occur (Orgel, 1967, p. 60; Burns, 1970, p. 22), experimental data nearly always show transition elements with  $d^4$  electronic configurations in octahedral coordination with four short coplanar bonds and two longer axial bonds (Orgel, 1967, p. 62). Norrishite has this configuration, which indicates that the  $d_{z^2}$  orbital is occupied. Other structures with  $Mn^{3+}$  octahedra such as manganite (Dachs, 1963) and groutite (Dent Glasser and Ingram, 1968), show distorted octahedra of this type. The ratios of the mean coplanar bond lengths to the mean axial bond lengths for norrishite, manganite, and groutite  $Mn^{3+}$  octahedra are 0.832, 0.849, and 0.855, respectively.

The Jahn-Teller distortions are reflected in a comparison of shared and unshared edge lengths. The two coplanar shared edge lengths, O(3)-O(3) and O(4)-O(4), are 2.71(1) Å and 2.52(2) Å, respectively, and are shorter than the shared edges associated with the axial anions, [O(3)-O(3)]<sub>x2</sub> and [O(4)-O(3)]<sub>x2</sub>, which are 2.86(1) Å and 2.94(1) Å, respectively. Similarly, the two coplanar unshared edges, O(3)-O(4), both 2.866 Å, are shorter than both O(3)-O(4) [3.08(1) Å] and O(3)-O(3)' [2.934(5) Å].

The apical O atoms of opposing tetrahedra within the 2:1 layer are linked by a diagonal edge, an edge that is shared also between M(1) and M(2). This edge determines the extent to which the intralayer shift deviates from the ideal of 0.333 $a$ . It is this intralayer shift that produces a stagger of the upper tetrahedral sheet relative to the lower tetrahedral sheet in  $b$ -axis projections of 2:1 layers. In addition, there is a layer offset, which is caused by the interlayer cation displaced from the center of the hexagonal ring. The intralayer shift and the layer offset vectors determine the  $\beta$  angle. For trioctahedral micas

TABLE 6. Calculated structural parameters for norrishite

Parameter	Value
$\alpha$ ( $^\circ$ )*	0.6
$\psi$ ( $^\circ$ )**	59.14 M(1)
	57.72 M(2)
$\tau_{tot}$ ( $^\circ$ )†	112.7
Sheet thickness‡	
octahedral (Å)	2.176
tetrahedral (Å)	2.254
Interlayer separation (Å)	3.275
$\beta_{ideal}$ ( $^\circ$ )§	100.09

\*  $\alpha = 1/2[120^\circ - \text{mean } O_T-O_T-O_b \text{ angle}]$ .

\*\*  $\psi = \cos^{-1}[\text{thickness}/2(M-O)]$ .

†  $\tau = \text{mean } O_T-T-O_m$ .

‡ Tetrahedral thickness includes O(4).

§  $\beta_{ideal} = 180^\circ - \cos^{-1}[a/3c]$ .

where the M(1) and M(2) sites are about equal in size, the intralayer shift is nearly ideal at  $-0.333a$ . In contrast, the dioctahedral micas of the  $1M$  polytype where M(1) is much larger than M(2), the effective intralayer shift is increased (Bailey, 1984, p. 33). This overshift along with a much smaller layer offset produces a  $\beta$  angle larger than the ideal by a couple of degrees. Although M(1) is larger than M(2) in norrishite, Jahn-Teller distortions require the O(3)-O(3) diagonal edge to be relatively short [2.71(1) Å], thereby producing an intralayer shift ( $-0.274a$ ) that is less than the ideal value. Because the layer offset is small ( $+0.002a$ ), the intralayer shift dominates and the  $\beta$  angle (98.22 $^\circ$ ) is smaller than the ideal of 100.09 $^\circ$  (Table 6).

### Dioctahedral-like distortions

A large cation of low valence in M(1) and a trivalent cation occupying the two M(2) sites is topologically analogous to the general dioctahedral structure. The observed range of unshared octahedral edge lengths given by Bailey (1984) for Al-rich dioctahedral micas is 2.7 Å–2.9 Å (vs. 3.0 Å–3.2 Å for trioctahedral micas). The O(3)-O(4) and O(3)-O(3)' unshared edges in norrishite are 2.866(6) Å and 2.934(5) Å, respectively.

Lee and Guggenheim (1981) observed that dioctahedral micas exhibit a shift of the apical O atoms approximately parallel to (001) in partial response to the longer unshared octahedral edges of the vacant M(1) site. A similar shift is observed in norrishite and reflects both the presence of the large Li cation in M(1) (instead of a vacancy) and Mn-Mn repulsion across the O(3)-O(3)' edge, by analogy to  $Al^{3+}$ - $Al^{3+}$  repulsions also causing this shift as suggested by Lee and Guggenheim (1981). Furthermore, in dioctahedral micas, the apical O shift is usually associated with basal O offsets of 0.1–0.2 Å, which form a corrugation of the basal plane along the [110] direction. This latter effect is limited in norrishite (0.058 Å) because the size differences between M(1) and M(2) are smaller than in most dioctahedral micas. The apical O shift, however, is reflected in the magnitudes of the  $O_{basal}$ -T- $O_{apical}$  bond angles which are 113.8 $^\circ$ , 112.6 $^\circ$ , and 111.7 $^\circ$  for O(1)-T-O(3) and the two O(2)-T-O(3) angles, respectively. The magnitudes of these angles and their opposing edges in-

**TABLE 7.** Structural parameters for polyolithionite, taeniolite, norrishite and "oxybiotite"

	Inter-layer separation (Å)	Si-O <sub>apical</sub> distance (Å)	$\tau_{\text{tet}}$ (°)	Tetra-hedral thickness (Å)
Synthetic polyolithionite* K(Li <sub>2</sub> Al)Si <sub>4</sub> O <sub>10</sub> F <sub>2</sub>	3.274	1.564	111.8	2.247
Synthetic taeniolite** K(Mg <sub>2</sub> Li)Si <sub>4</sub> O <sub>10</sub> F <sub>2</sub>	3.297	1.586	112.7	2.251
Norrishite† K(Mn <sup>3+</sup> Li)Si <sub>4</sub> O <sub>10</sub>	3.275	1.571	112.7	2.252
"Oxybiotite-1M"‡ (K <sub>0.77</sub> Na <sub>0.16</sub> Ba <sub>0.02</sub> )(Mg <sub>1.87</sub> Al <sub>0.16</sub> - Fe <sub>0.86</sub> Ti <sub>0.34</sub> Mn <sub>0.01</sub> )(Si <sub>2.84</sub> - Al <sub>1.16</sub> )O <sub>11.82</sub> (OH) <sub>0.21</sub> F <sub>0.17</sub>	3.287	1.668	110.2	2.275

\* Takeda and Burnham (1969).  
 \*\* Toraya et al. (1977).  
 † This study.  
 ‡ Ohta et al. (1982).

dicate that O(3) and O(3)' approach each other along their shared edge.

Tetrahedral distortion in norrishite reflects the trends observed in micas as a whole, in that pyramidal edges are larger than basal edges (Takéuchi, 1975) and thus tetrahedra are elongated perpendicular to the basal plane. The mean of all six edges (2.683 Å) is greater than the mean of the three basal edges (2.610 Å); the basal face is contracted, reducing the lateral dimensions of the sheet. Tetrahedral distortion,  $\tau_{\text{tet}}$ , defined as the mean of the three O<sub>basal</sub>-T-O<sub>apical</sub> angles is 112.7° (Table 6), the largest value observed among the naturally occurring micas. This value suggests significant tetrahedral elongation, as an increase of  $\tau_{\text{tet}}$  relative to the ideal value of 109°28' is usually associated with an increase in sheet thickness. However, the magnitude of  $\tau_{\text{tet}}$  may be related also to the short Si-O<sub>apical</sub> bond distance as well as the O<sub>basal</sub>-T-O<sub>apical</sub> bond angles discussed above. The short Si-O(3) distance of 1.571 Å is similar to that observed in synthetic fluorine end-member polyolithionite (Takeda and Burnham, 1969). These authors attributed the 1.564 Å distance in that phase to local imbalance of electrostatic valence, where apical O atoms are coordinated to two Al<sup>3+</sup> and Li<sup>+</sup>. An analogy exists with norrishite, with each apical O atom [O(3)] coordinated to two Mn<sup>3+</sup> in M(2) and one Li<sup>+</sup> in M(1). One Mn is displaced away from O(3) as the result of the strong attraction to O(4), whereas the other is coordinated to O(3) along the extended axial bond of the octahedra as governed by the Jahn-Teller effect. Hence, the increased bond lengths produce a charge deficiency on the apical O atom. In compensation, the tetrahedral cation is displaced toward O(3) along *c*\*. Such a displacement is reflected in larger O<sub>basal</sub>-T-O<sub>apical</sub> angles and smaller O<sub>basal</sub>-T-O<sub>basal</sub> angles, compared to ideal values. The means of these angles are 112.7° and 106.0°, respectively. The large difference probably reflects the combined effects of cation displacement and compression within the (001) plane.

In mica structures, there is a misfit between the lateral

dimensions of the octahedral and tetrahedral sheets, with the tetrahedral sheet generally being larger. To compensate, adjacent tetrahedra within a silicate ring rotate in opposite directions by an amount  $\alpha$ , which reduces the lateral dimensions of the sheet. In norrishite, the tetrahedral rotation is 0.6°, the lowest value observed among the micas, and the tetrahedral rings are essentially hexagonal (Fig. 1). Lack of misfit results from the combined effects of octahedral flattening ( $\psi$ ), expansion of the octahedral sheet due to the large Li<sup>+</sup> and Mn<sup>3+</sup>, a Si-rich tetrahedral sheet, and compression of individual tetrahedra within (001).

### Interlayer separation

The interlayer separation in micas depends partly on coulombic interactions between the interlayer cation and the adjacent negatively charged F<sup>-</sup> or OH<sup>-</sup> (McCauley et al., 1973; Ohta et al., 1982). In OH-rich structures, the proton reduces the interlayer cation to O attraction, whereas in F-rich structures the absence of H results in a strong attraction. Consequently, F-rich structures tend to have narrow interlayers. The site usually associated with F<sup>-</sup> or OH<sup>-</sup> in other micas contains a divalent anion (O<sup>2-</sup>) in norrishite [designated as O(4)], thereby creating a greater attraction with K. The 3.275 Å interlayer separation in norrishite approaches the lower limit of observed values in trioctahedral micas, supporting the role of OH<sup>-</sup>, F<sup>-</sup>, and O<sup>2-</sup> as an important influence on interlayer separation. Similarly, McCauley et al. (1973) reported variations in interlayer separation of 3.36 Å and 3.62 Å for fluorine end-member phlogopite and phlogopite, respectively, and Ohta et al. (1982) showed that partial hydrogenation of "oxybiotite" resulted in an increase in interlayer separation from 3.287 Å to 3.334 Å.

Interlayer separations (Table 7) are compared for four trioctahedral micas that exhibit the narrowest interlayers among the K-rich varieties: norrishite, synthetic taeniolite (Toraya et al., 1977), synthetic fluorine end-member polyolithionite (Takeda and Burnham, 1969), and "oxybiotite-1M," (Ohta et al., 1982). Norrishite is analogous to taeniolite and polyolithionite with respect to a relatively short Si-O<sub>apical</sub> bond distance (as discussed above), the  $\tau_{\text{tet}}$  angle, and the tetrahedral sheet chemistry, and to "oxybiotite" with respect to O in O(4). It is noteworthy that norrishite and polyolithionite have identical interlayer spacings, although the site analogous to O(4) in polyolithionite is occupied by F. This observation suggests that 3.27 Å may be the limit for the approach between two adjacent Si-rich tetrahedral sheets in micas, due to the Si-Si repulsion across the interlayer. If such a limit exists, then the displacement of Si along *c*\* which results in a short Si-O<sub>apical</sub> distance, is favored also, and thus may be caused partially by Si-Si repulsion.

In contrast to the observed interlayer separations, it might be expected that "oxybiotite" would have a narrower interlayer than that of taeniolite or polyolithionite because of the -2 charge associated with O in O(4). However, tetrahedral Al in "oxybiotite" enlarges the tetrahe-

dral sheet both vertically and laterally; thus, the increased distance between K and O in O(4) minimizes attraction in comparison to a structure with a Si-rich tetrahedral sheet. In addition, repulsion between tetrahedral cations is reduced with the substitution of Al for Si. This may explain why "oxybiotite," which exhibits a similar displacement of M(2) away from O(3) (as in norrishite), lacks a compensating displacement of Si toward O(3).

### CONCLUSION

Studies involving the substitution of Fe<sup>3+</sup> for Fe<sup>2+</sup> in synthetic annite and biotite (Wones, 1963; Wones and Eugster, 1965; Parten et al., 1983), which may be coupled with O in O(4), related the reaction  $R^{2+} + OH^- = R^{3+} + O + H$  to thermal stability, physical properties, and  $f_{O_2}$ , but not to the possible structural effects of such a substitution. Although this reaction may not be appropriate to norrishite, the results presented here allow a better understanding of both the localized atomic arrangement around the highly undersaturated O position found in "oxymicas," and the effect of this arrangement on polyhedral distortion, interlayer separation, and charge-balance summations for "oxymicas" in general. The localized atomic adjustments associated with this highly undersaturated O position help stabilize the structure, which is clearly less stable with respect to more ideal trioctahedral micas with OH or F. However, because octahedral distortions are influenced by the Jahn-Teller effects associated with Mn<sup>3+</sup>, some of these results may not apply in detail to Fe<sup>3+</sup>-rich structures, which are not affected by Jahn-Teller distortions. Theoretically, it should be possible to synthesize an Fe analogue of norrishite, as the ionic radii of Fe<sup>3+</sup> and Mn<sup>3+</sup> are equal (Shannon, 1976); such a structure would be free from Jahn-Teller distortions, thereby making a comparison to norrishite of interest.

### ACKNOWLEDGMENTS

We thank R.A. Eggleton, Australian National University, for kindly providing norrishite for this study, and S.W. Bailey, University of Wisconsin-Madison, and J.M. Hughes, Miami University, Ohio, for reviewing the manuscript. Support for this work was made available by the Petroleum Research Fund, administered by the American Chemical Society under grant 21974-AC8-C and by the Experimental and Theoretical Geochemistry Program of the National Science Foundation under grants EAR87-04681 and EAR90-03688.

### REFERENCES CITED

- Ashley, P.M. (1986) An unusual manganese silicate occurrence at the Hoskins mine, Grenfell district, New South Wales. *Australian Journal of Earth Sciences*, 33, 443-456.
- Bailey, S.W. (1984) Crystal chemistry of the true micas. In *Mineralogical Society of America Reviews in Mineralogy*, 13, 13-57.
- Brown, I.D. (1977) Predicting bond lengths in inorganic crystals. *Acta Crystallographica*, B33, 1305-1310.
- Brown, I.D., and Shannon, R.D. (1973) Empirical bond strength-bond length curves for oxides. *Acta Crystallographica*, A29, 266-287.
- Burns, R.G. (1970) *Mineralogical applications of crystal field theory*. Cambridge University Press, Cambridge, England.
- Busing, W.R., Martin, K.O., and Levy, H.A. (1962) ORFLS, a Fortran crystallographic least-squares refinement program. U.S. National Technical Information Service ORNL-TM-305.
- Busing, W.R., Martin, K.O., and Levy, H.A. (1964) ORFFE, a Fortran crystallographic function and error program. U.S. National Technical Information Service ORNL-TM-306.
- Cromer, D.T., and Mann, J.B. (1968) X-ray scattering factors computed from numerical Hartree-Fock wave functions. *Acta Crystallographica*, A24, 321-324.
- Dachs, H. (1963) Neutronen- und Röntgenuntersuchungen am Manganit, MnOOH. *Zeitschrift für Kristallographie*, 118, 303-326.
- Dent Glasser, L.S., and Ingram, L. (1968) Refinement of the crystal structure of groutite,  $\alpha$ -MnOOH. *Acta Crystallographica*, B24, 1233-1236.
- Eggleton, R.A., and Ashley, P.M. (1989) Norrishite, a new manganese mica,  $K(Mn^{3+}Li)Si_4O_{13}$ , from the Hoskins mine, New South Wales, Australia. *American Mineralogist*, 74, 1360-1367.
- Guggenheim, S. (1981) Cation ordering in lepidolite. *American Mineralogist*, 66, 1221-1232.
- Larsen, E.S., Irving, J., Gonyer, F.A., and Larsen, E.S. III (1937) Petrologic results of a study of the minerals from the Tertiary volcanic rocks of the San Juan region, Colorado. *American Mineralogist*, 22, 898-905.
- Lee, J.H., and Guggenheim, S. (1981) Single crystal X-ray refinement of pyrophyllite-1Tc. *American Mineralogist*, 66, 350-357.
- McCaughey, J.W., Newnham, R.E., and Gibbs, G.V. (1973) Crystal structure analysis of synthetic fluorophlogopite. *American Mineralogist*, 58, 249-254.
- North, A.C.T., Phillips, D.C., and Matthews, F. (1968) A semi-empirical method of absorption correction. *Acta Crystallographica*, A24, 351-359.
- Ohta, T., Takeda, H., and Takéuchi, Y. (1982) Mica polytypism: Similarities in the crystal structures of coexisting 1M and 2M, oxybiotite. *American Mineralogist*, 67, 298-310.
- Orgel, L.E. (1967) *An introduction to transition-metal chemistry: Ligand field theory*. Methuen, London.
- Parten, E., Hewitt, D.A., and Wones, D.R. (1983) Quantification of ferric iron in biotite. *Geological Society of America Abstracts with Programs*, 15, 659.
- Shannon, R.D. (1976) Revised effective ionic radii and systematic studies of interatomic distances in halides and chalcogenides. *Acta Crystallographica*, A32, 751-892.
- Takeda, H., and Burnham, C.W. (1969) Fluor-polyolithionite: A new lithium mica with nearly hexagonal  $(Si_2O_3)^{2-}$  ring. *Mineralogical Journal (Japan)*, 6, 102-109.
- Takéuchi, Y. (1975) The distortion of Si(Al)-tetrahedra in sheet silicates. In K. Henmi, Ed., *Contributions to clay mineralogy*, T. Sudo volume, 1-6.
- Toraya, H., Iwai, S., Marumo, F., and Hirao, M. (1977) The crystal structure of taeniolite,  $KLiMg_2Si_4O_{10}F_2$ . *Zeitschrift für Kristallographie*, 146, 73-83.
- Wones, D.R. (1963) Physical properties of synthetic biotites on the join phlogopite-annite. *American Mineralogist*, 48, 1300-1321.
- Wones, D.R., and Eugster, H.P. (1965) Stability of biotite: Experiment, theory and application. *American Mineralogist*, 50, 1228-1272.

MANUSCRIPT RECEIVED JUNE 11, 1990

MANUSCRIPT ACCEPTED NOVEMBER 9, 1990